

# Currents, Torques, and Polarization Factors in Magnetic Tunnel Junctions

J. C. Slonczewski<sup>1</sup>

IBM Watson Research Center, Box 218, Yorktown Heights,  
NY 10598 USA

February 20, 2019

## Abstract

Application of Bardeen's tunneling theory to magnetic tunnel junctions having a general degree of atomic disorder reveals the close relationship between magneto-conduction and voltage-driven pseudo-torque, as well as the thickness dependence of tunnel-polarization factors. Among the results: 1) The torque generally varies as  $\sin \theta$  at constant applied voltage. 2) Whenever polarization factors are well defined, the voltage-driven torque on each moment is uniquely proportional to the polarization factor of the other magnet. 3) At finite applied voltage, this relation predicts significant voltage-asymmetry in the torque. For one sign of voltage the torque remains substantial even when the magnetoconductance is greatly diminished. 4) A broadly defined junction model, called *ideal middle*, allows for atomic disorder within the magnets and F/I interface regions. In this model, the spin- $\sigma$  dependence of a basis-state weighting factor proportional to the sum over general state index  $p$  of  $(\int \int dy dz \Psi_{p,\sigma})^2$  evaluated within the (e.g. vacuum) barrier generalizes the local state density in previous theories of the tunnel-polarization factor. 5) For small applied voltage, tunnel-polarization factors remain legitimate up to first order in the inverse thickness of the ideal middle. An algebraic formula describes the first-order corrections to polarization factors in terms of newly defined lateral auto-correlation scales.

---

<sup>1</sup>IBM RSM Emeritus

# 1 Introduction

When first predicted, voltage-driven pseudo-torque in magnetic tunnel junctions (MTJs) appeared to be a marginal effect [1]. The resistances of early experimental tunneling barriers appeared too large to permit anything more than a very small torque. Resistive heating of the MTJ would have limited the possibilities to only a small voltage-driven decrease of linewidth of narrowly-focussed Brillouin-scattering. (This prediction was never tested.) As a result, one could not yet predict anything as remarkable as the now well-established magnetic reversal and high-frequency precession observed when the resistive barrier is replaced by a *metallic* spacer. For recent experimental work and other references dealing with current-driven oscillations and switching involving metallic spacers, see Refs. [2] and [3].

But in recent years, experimental activity in tunneling magnetoresistance has expanded vastly. It is fueled in great part by the experimental discovery of substantial tunneling magnetoresistance [4] at room-temperature and the resulting intensive exploration of non-volatile magnetic memory reviewed recently [5]. A part of this activity is the search for junction compositions and deposition techniques which lower the resistance to values more suitable for integrated-circuit application. Indeed, there now exist very recent experimental reports of current-driven switching in MTJs [6],[7]. This development may make possible two-terminal memory elements avoiding resort to three-terminal devices using a metallic spacer for switching and a tunnel barrier for reading [8].

According to recent reviews of tunneling magneto-conductance [9],[10],[11],[12], empirical ferromagnet polarization coefficients  $P_i$  ( $i = \text{L,R}$  refer to left and right magnets  $F_i$  in Fig. 1a) measured with  $F_i\text{IS}$  junctions having a superconducting counter electrodes [13] account well for magnetoresistance in FIF junctions. Let the formula

$$J(V, \theta) = -J_0(V)[1 + \iota(V) \cos \theta], \quad \text{with } J_0 > 0 \text{ for } V > 0 \quad (1)$$

for current density at constant applied voltage  $V$  define the coefficient  $\iota$  of magneto-conduction. Here  $\theta$  is the angle between the moments. (The  $-$  sign occurs in Eq. (1) because of the convention in Fig. 1 where particle-number current is positive for  $V > 0$ .) In this article, the coefficient  $\iota$  is more convenient than the experimentally preferred low-voltage tunneling-magnetoresistance ratio

$$\text{TMR} = (R_{\text{AP}} - R_{\text{P}})/R_{\text{P}} = 2\iota/(1 - \iota). \quad (2)$$

The original formula of Julliere [14], expressed in our notation by the formula,

$$\iota = P_{\text{L}}P_{\text{R}}, \quad (3)$$

enjoys considerable success in interpreting experiments [9]. We find below that whenever  $\iota$  separates this way into two polarization factors characteristic of the respective electrode-and-barrier compositions, pseudo-torque expressions having coefficients  $\tau_L$  and  $\tau_R$ , whose simplicity parallels that of Eqs.(1) and (3), hold also.

However, theory does not *generally* support the separability of spin-channel currents into the right-dependent and left-dependent factors needed to justify polarization factors in the first place. Previous theories attack the question of polarization coefficients within the context of real electron structure by considering the transmission of electrons initially occupying well-defined crystalline-momentum states [15],[16],[17]. They posit either complete absence of disorder or disorder only within the barrier to legitimize tunnel-polarization factors.

However multiple scattering, which causes resistivity, abounds within the electrodes. A new feature of the present work is to forego altogether crystal-momentum quantization within the electrodes. This feature is particularly appropriate to current experiments relying typically on sputtered magnetic elements and alloys having high defect concentration[2],[3]. Both alloying and structural defects may cause an electron to scatter many times before it tunnels across the barrier. Our elastic-tunneling theory rests on Bardeen's transfer-hamiltonian formula [18],[19], which is applicable to tunneling transitions between thermal baths of electron states without any spatially conserved observables.

Our model of the junction, called *ideal middle*, excludes disorder only from a central slab of uniform thickness  $w$ , which may consist of vacuum or crystal lying somewhere within the barrier. We find that exact factorization, expressed by Eq.(3), occurs only in the limit  $w \rightarrow \infty$ , just as in the absence of disorder. Further, our parametrization of lateral *autocorrelation* of the Bardeen basis function sets predicts well-defined tunneling-polarization factors to first order in  $w^{-1}$ , which enhances their legitimacy for interpretation of experiments for any degree of disorder. Calculations and measurements of the new correlation-scale parameters  $\xi_\sigma$  could shed quantitative light on the genesis of polarization factors.

By way of organization, Section 1 is this Introduction and Section 2 shows how spin-channel tunnel currents generally determine voltage-driven torque. Section 3 derives the resulting fully general expressions for the magnetoelectronic coefficients  $\iota$ ,  $\tau_L$ , and  $\tau_R$ . Section 4 shows how tunneling-polarization factors and the resulting simple expressions for  $\iota$ ,  $\tau_L$ , and  $\tau_R$  arise from a formal separability condition. Section 5 addresses the expressions for unsymmetrical torque arising from finite-voltage dependence of polarization factors. Section 6 derives the separation condition and tunneling-polarization factors which arise in the ideal-middle model at  $w \rightarrow \infty$ . Section 7 presents a procedure for expanding magnetic tunneling properties for finite  $w$

and derives a formula for the first-order thickness dependence of tunnel-polarization factors. Section 8 summarizes and discusses the results.

## 2 First currents, then pseudo-torques

Whenever two ferromagnets are separated by a nonmagnetic spacer, whether a tunneling barrier or a metal, exchange-generated pseudo-torques acting on the magnetic moments are attributable to the flow of spin-polarized current. [For a discussion of the genesis of pseudo- (or effective-) torque from the principle of spin continuity, see Appendix B of Ref. [20].] Consider particularly the series electric circuit in Fig. 1a in which an external voltage source  $V$  causes electric-current density  $J$  to flow in series through a left metallic ferromagnetic film  $F_L$ , a thin insulator  $I$  serving as a tunnel barrier, and finally a grounded right metallic ferromagnetic film  $F_R$ . By assumption, in our continuous picture the *direction* of spontaneous magnetization  $\mathbf{M}_L(x) = -M_L(x)\mathbf{l}$  within  $F_L$  does not depend on the plane-perpendicular coordinate  $x$ ; similarly  $\mathbf{M}_R(x) = -M_R(x)\mathbf{r}$  within  $F_R$ . (Here the three-dimensional unit vectors  $\mathbf{l}$  and  $\mathbf{r}$  include the angle  $\theta = \cos^{-1} \mathbf{r} \cdot \mathbf{l}$ .) Thus we lay aside the possibilities of spin-wave excitations [21] and the volume-intensive pseudo-torque [22] arising from dependence of magnetization direction on  $x$  which become significant for larger film thickness and current density when the spacer is metallic..

One goal is to calculate the component  $T_R$  of interfacial pseudo-torque vector  $\mathbf{T}_R$  per unit area, acting on  $\mathbf{M}_R$ , which lies orthogonal to  $\mathbf{r}$  *within the instantaneous plane* common to  $\mathbf{l}$  and  $\mathbf{r}$  as indicated in Fig. 1a. (The magnetic space spanned by  $\mathbf{l}$  and  $\mathbf{r}$  is completely separate from position space  $x, y, z$ .) A general expression for  $T_R$  reads thus:

$$T_R = \hbar[J_{L,+} - J_{L,-} + (J_{R,-} - J_{R,+}) \cos \theta]/2e \sin \theta \quad (4)$$

The left spin-channel electric current densities  $\mathbf{J}_{L,\pm} = J_{L,\pm}\mathbf{l}$  flow through plane A (See below) in direction  $x$  and the right  $\mathbf{J}_{R,\pm} = J_{R,\pm}\mathbf{r}$  flow through plane B. The factor  $-\hbar/2e$  converts any electric channel current to one of spin momentum. A similar expression holds for the pseudo-torque  $T_L$  on the left moment. The torques  $T_R$  and  $T_L$  must generally be included in the dynamical Landau-Lifshitz equations for the two magnetic films.

Although previously applied only to all-metallic multilayers [23],[20], Eq. (4) holds equally well when the spacer is an insulator. For its derivation, one posits the non-relativistic  $n$ -electron hamiltonian, including just kinetic energy and coulomb terms due to external voltage and electron-nuclear and electron-electron interactions.

In addition, one accepts the microscopically-based approximation, defensible in the case of Co, that the transverse (to local  $\mathbf{M}$ ) components of conduction-electron spin polarization created at the two internal I/F interfaces decay to zero well within a characteristic distance  $d_{\perp} \approx 1\text{nm}$  [20], estimated explicitly for Co by a scattering calculation [24]. Moreover, in one experiment the threshold current for switching of Co by polarized current flowing through a *metallic* spacer is simply proportional to film thickness down to 1 nm, confirming that the transverse polarization inside the ferromagnetic film vanishes at this scale [25]. Therefore the currents in the left and right magnets must be polarized along instantaneous left ( $\mathbf{l}$ ) and right ( $\mathbf{r}$ ) moment axes at depths greater than  $d_{\perp}$  from the F/I interfaces.

In the extensive literature on tunneling magnetoresistance involving Fe, Co, Ni and magnetically concentrated alloys of these elements there is little indication of spin relaxation at I/F interfaces. Moreover experiments at cryogenic temperatures reveal that the distance  $\lambda_{\parallel}$  of spin relaxation due to spin-orbit coupling for the polarization component along the axis  $\mathbf{M}$  is about 50 nm for Co and about 5.5 nm for Ni-Fe[26]. Thus it follows that, at least in the case of Co where  $\lambda_{\parallel} \gg d_{\perp}$ , the channel currents  $J_{L,\pm}$  and  $J_{R,\pm}$  should be evaluated at the planes A and B lying at the distance  $d_{\perp}$  from the respective F/I interfaces. For within the space between these planes one may neglect spin-orbit effects and embrace the well-known spin-continuity relation which equates the sum of equivalent interfacial pseudo-torques with the net inflow of spin current [23],[20] having polarizations  $\mathbf{l}$  and  $\mathbf{r}$  respectively. In the notation of Fig. 1a, the statistical average of this equality becomes

$$\mathbf{T}_L + \mathbf{T}_R = \frac{\hbar}{2e} [(J_{L,-} - J_{L,+})\mathbf{l} + (J_{R,+} - J_{R,-})\mathbf{r}]. \quad (5)$$

Since  $\mathbf{l} \cdot \mathbf{T}_L = 0$ , the scalar product of Eq. (5) with  $\mathbf{l}$  eliminates  $\mathbf{T}_L$  and gives Eq. (4) for the magnitude  $T_R$ . A similar equation holds for  $T_L$ .

The above argument neglects a *spatially oscillating* transverse current, calculated in certain FNF cases lie between 0 and  $\simeq 10\%$  of the incident spin current (See Fig. 7 of Ref. [24]), and is likely due to interferences at the perfect interface assumed in the calculation. This amount will be decreased by irregularities at real interfaces.

Even in the *absence of applied electric voltage* ( $V = 0$ ) an additional *perpendicular* component of exchange pseudo-torque  $\mathbf{T}_{R\perp} = K\mathbf{l} \times \mathbf{r} = -\mathbf{T}_{L\perp}$  predicted for MTJs [1], is generally related to conventional coupling energy  $-K\mathbf{l} \cdot \mathbf{r} = -K \cos \theta$ . It must also be included in the Landau-Lifshitz equation for the dynamics of magnet  $\mathbf{F}_R$ . However, in that toy rectangular-barrier MTJ model, the dependence of  $\mathbf{T}_{R\perp}$  and  $\mathbf{T}_{L\perp}$  on applied voltage occurred only in higher order ( $\propto V^2$ ) than the torque given by Eq. (4) ( $\propto V$ ). Moreover, its dynamic effect is relatively weaker in structures

with coincident easy anisotropy axes and low magnetic damping, such as the pillars using metallic spacers experimentally favored for efficient current-driven switching [2]. In addition, the Bardeen tunneling theory used here does not readily provide this out-of-plane pseudo-torque. For these reasons, we do not attempt to predict the perpendicular pseudo-torque component in this work.

### 3 Magneto-conduction and pseudo-torques

Equation (4) effectively reduces the interacting-electron problem of voltage-driven pseudo-torque to the customarily independent-electron problem of spin-channel currents. One recently reviewed theory of collinear MTJ magnetoresistance [11] extends naturally to tunneling between spin channels for general  $\theta$ . For adaptation of the Bardeen transfer-hamiltonian tunneling theory [18],[19] to the MTJ of Fig. 1a, a stationary basis state within the electron reservoir  $F_L$  has orbital index  $p$  and majority/minority spin  $\sigma = \pm$  quantized along axis  $\mathbf{l}$ . It satisfies  $(H + eV - \epsilon_{p,\sigma})|p, \sigma\rangle = 0$ , and decays exponentially within the barrier, considered semi-infinite in width when defining the basis states. Here,  $H = p^2/2m + \Sigma_\sigma |\sigma\rangle U_\sigma(x, y, z) \langle\sigma|$ , where the potential  $U_\sigma$ , depends on spin within the ferromagnets according to itinerant-electron magnetism theory [27], but not in the barrier. Within  $F_R$ , a similar state satisfies  $(H - \epsilon_{q,\sigma'})|q, \sigma'\rangle = 0$  with quantization axis  $\mathbf{r}$ . Because the barrier is assumed to dominate all other resistances of this circuit, the spin channels are shown in Fig. 1b as shorted in each magnet and/or external-contact region by spin lattice relaxation due to spin-orbit coupling. One may disregard *spin accumulation* and the related distinction between electric and electrochemical potentials which are important when a non-magnetic metallic spacer substitutes for the barrier[28].  $U_\sigma$  includes all elastic terms arising from atomic disorder due to alloying, defects, interfacial atomic interdiffusion, etc. The state indices  $p, q$  simply enumerate the exact eigenstates  $|p, \sigma\rangle, |q, \sigma'\rangle$  of  $H$  in the Bardeen basis. Each such state incorporates effects of all multiple elastic scatterings without limit.

Employing the spinor transformation connecting quantization axes  $\mathbf{l}$  and  $\mathbf{r}$ , the transfer matrix element takes the form

$$\langle p, \sigma | H - \varepsilon | q, \sigma' \rangle = \begin{bmatrix} \gamma_{p,+,q,+} \cos \frac{\theta}{2} & \gamma_{p,+,q,-} \sin \frac{\theta}{2} \\ -\gamma_{p,-,q,+} \sin \frac{\theta}{2} & \gamma_{p,-,q,-} \cos \frac{\theta}{2} \end{bmatrix}. \quad (6)$$

Bardeen [18] gives the expression

$$\gamma_{p,\sigma;q,\sigma'}(x) = \frac{-\hbar^2}{2m} \int dy dz (\psi_{p,\sigma} \partial_x \varphi_{q,\sigma'} - \varphi_{q,\sigma'} \partial_x \psi_{p,\sigma}), \quad (7)$$

where the integral is over unit area for coordinate  $x$  lying appropriately (see below) inside the barrier. The energies  $\epsilon_{p,\sigma}$  and  $\epsilon_{q,\sigma'}$  may differ only infinitesimally from the Fermi value  $\epsilon = \epsilon_F$ . The hamiltonian  $H$ , the left ( $\psi_{p,\sigma}$ ) and right ( $\varphi_{q,\sigma'}$ ) orbital wave functions, and these matrix elements (7) are real.

Only the neglect of cross-barrier overlaps  $\langle p, \sigma | q, \sigma' \rangle$  allows use of the Fermi golden rule of perturbation theory which is strictly valid for an orthonormal basis. Substitution of the perturbation (6) into this rule is followed by summation over the initial states in an infinitesimal energy band of width  $eV$ . Thus the partial electric current density flowing between channel  $\sigma$  in  $F_L$  and channel  $\sigma'$  in  $F_R$  becomes

$$J_{\sigma,\sigma'} = \frac{-2\pi e^2 V}{\hbar} \sum'_{p,q} \langle p, \sigma | H - \epsilon_F | q, \sigma' \rangle^2. \quad (8)$$

at  $T = 0$  K. The  $'$  in  $\sum'_{p,q}$  imposes the conditions  $\epsilon_F < (\epsilon_{p,\sigma}, \epsilon_{q,\sigma'}) < \epsilon_F + eV$ .

Notations in the equivalent circuit shown in Fig. 1b make plain the relations

$$J_{L\sigma} = J_{\sigma,+} + J_{\sigma,-}, \quad J_{R\sigma'} = J_{+,\sigma'} + J_{-,\sigma'}, \quad (\sigma, \sigma' = \pm) \quad (9)$$

needed in Eq. (4). The right hand sides of these equations are evaluated from Eqs. (6-8).

Next we write the total electric current density  $J = J_{L,+} + J_{L,-}$ . With the notation

$$\Gamma_{\sigma,\sigma'} = \frac{2\pi eV}{\hbar} \sum'_{p,q} \gamma_{p,\sigma;q,\sigma'}^2 \quad (10)$$

for particle-number interchannel tunneling current with the angular factor omitted, the above equations combine to give Eq. (1) with

$$J_0 = e(\Gamma_{+,+} + \Gamma_{-,-} + \Gamma_{+,-} + \Gamma_{-,+})/2 \quad (11)$$

and the magneto-conduction coefficient

$$\iota = e(\Gamma_{+,+} + \Gamma_{-,-} - \Gamma_{+,-} - \Gamma_{-,+})/2J_0. \quad (12)$$

Eq.(4) becomes

$$T_R = -(\hbar\tau_R J_0/2e) \sin \theta \quad (13)$$

or, in coordinate-free form

$$\mathbf{T}_R = (\hbar\tau_R J_0/2e) \mathbf{r} \times (\mathbf{l} \times \mathbf{r}), \quad (14)$$

with the torque coefficient

$$\tau_R = e(\Gamma_{+,+} + \Gamma_{+,-} - \Gamma_{-,-} - \Gamma_{-,+})/2J_0. \quad (15)$$

The fact that the linear combination of the parameters  $\Gamma_{\sigma,\sigma'}$  appearing in Eq. (12) differs from that in Eq. (15) and a similar one for  $\mathbf{T}_L$  precludes any fully general connection between torques and electrical current.

## 4 Left-right separability

Particularly interesting relations arise if the summation in Eq. (10) happens to separate into left- and right-dependent factors giving rise to the form

$$\Gamma_{\sigma,\sigma'} = f\Omega_{L,\sigma}\Omega_{R,\sigma'} \quad (16)$$

Here the function  $f$ , which we make no attempt to evaluate, is independent of  $\sigma, \sigma'$ . (Sections 6 and 7 address conditions for this separability.) For then Eq. (11) gives

$$J_0 = \frac{ef}{2}(\Omega_{L,+} + \Omega_{L,-})(\Omega_{R,+} + \Omega_{R,-}), \quad (17)$$

and *tunneling polarization* parameters

$$P_i = \frac{\Omega_{i,+} - \Omega_{i,-}}{\Omega_{i,+} + \Omega_{i,-}} \quad (i = L, R) \quad (18)$$

which are directly measurable using FIS junctions[9]. In these terms, Eqs. (1) and (3) give the current-density and Eq. (14) the pseudo-torque with

$$\tau_R = P_L. \quad (19)$$

Similarly, the pseudo-torque on the left magnet is

$$\mathbf{T}_L = \frac{\hbar\tau_L}{2e}J_0\mathbf{l} \times (\mathbf{r} \times \mathbf{l}), \quad \tau_L = P_R. \quad (20)$$

The Eqs.(3) and (18)-(20) show the very close relation between current-driven torques and magneto-conduction at the same voltage if the separability condition (16) is satisfied.

The ground-breaking paper of Julliere[14] gave equations consistent with (3) and (18) taking  $\Omega_{L,\sigma}$  and  $\Omega_{R,\sigma'}$  to be spin-dependent basis-state densities at  $\varepsilon = \varepsilon_F$ . It appeared to attribute the dimensionless magneto-current coefficient  $\iota = P_L P_R$  to bulk properties of the two magnetic compositions involved. But the analytically solved free-electron rectangular-potential model [1] shows that an interface-dependent factor must be included in  $\Omega_{i,\sigma}$  as well. The transfer-hamiltonian treatment of this toy model follows immediately from the spinless treatment [29] giving

$$\Omega_{i,\sigma} = k_{i,\sigma}/(\kappa_0^2 + k_{i,\sigma}^2) \quad (21)$$

where

$$k_{i,\sigma}^2 = 2mE_{i,\sigma}/\hbar^2 \quad \text{and} \quad \kappa_0^2 = 2mB/\hbar^2. \quad (22)$$



Here,  $E_{i,\sigma}$  is the kinetic energy at the Fermi level and  $B$  is the barrier potential measured from the Fermi level. Equation (18) now gives

$$P_i = \frac{k_{i,+} - k_{i,-}}{k_{i,+} + k_{i,-}} \cdot \frac{\kappa_0^2 - k_{i,+}k_{i,-}}{\kappa_0^2 + k_{i,+}k_{i,-}} \quad (23)$$

in agreement with Ref. [1]. In this formula, the first factor depends purely on basis-state densities in the magnet, while the second mixes magnet and barrier properties. The results of the toy model [1] satisfy the general magneto-conduction relations (1), (3) and torque relations 14,19,20 with this substitution.

We note in passing that experimental variation of barrier height  $B$  (for small  $V$ ) shows considerable support for the zero of  $\iota$  at the barrier potential satisfying  $\kappa_0^2 - k_{i,+}k_{i,-} = 0$  expected from Eq. (23) [30]. Therefore, in spite of its fundamental naivete, this toy model enjoys some degree of credibility. It illustrates the general fact that, even when separability holds, each polarization factor is a property of the electron structure of the magnet and barrier *combination* as demonstrated by many experiments and calculations. Section 7 will discuss how deviations from Eq.(16) and the general tunnel-polarization picture may vary with barrier thickness.

## 5 Finite bias and torque asymmetry

In experiments, TMR typically decreases significantly with increasing finite  $V$  [9]. Voltage-dependence of interfacial transmission, special state density distributions, extrinsic impurity effects, and inelastic tunneling contribute to this decrease [9],[12]. This is important because large voltages will be required to read and write in a memory element.

The toy polarizations of Eq. (23) will serve to illustrate qualitatively the very unsymmetrical effect of finite  $V$  on voltage-driven pseudo-torque. One calculation of TMR uses the WKB approximation for the free-electron wave function within the constant-slope barrier potential sketched in Fig. 2 [31]. The interfacial transmissions are approximated by those of the flat-potential polarizations (23). The authors cite some experimental support for their results.

It is the decrease of  $P_i$  in the particular electrode which *collects* the tunneled electrons that primarily accounts for the decrease of  $\iota$  in the calculated result [31]. In Fig. 2, for  $V > 0$ , the collecting electrode lies on the right. Note that the electrons whose energy lies in a narrow band (shaded in Fig. 2) just below the Fermi level of the emitting electrode on the left of the barrier dominate the tunneling current because of the strong energy dependence of the WKB factor  $\exp[-2 \int \kappa(x)dx]$  in

the transmission coefficient. Since these hot electrons lie an amount close to above the Fermi level on the right, this energy shift  $eV$  must be taken into account when estimating  $P_R$ .

We simplify this model one step further and neglect the width of the shaded current band in Fig. 2. It is then clear that Eqs. (22) and (23) with  $i = L$  are still correct for  $P_L$ , neglecting correction for the finite slope of the barrier potential. However, the equations

$$k_{R\sigma}^2 = 2m(E_{R\sigma} + eV)/\hbar^2 \quad \text{and} \quad \kappa_0^2 = 2m(B - eV)/\hbar^2, \quad (24)$$

obtained by adding  $eV$  to each electron energy on the right, must replace Eqs.(22) for  $i = R$ . The conclusion is that the *collector* electrode is the one whose change (decrease, usually) is primarily responsible for the reduction, well known in experiments [9], of TMR with increasing  $V$ .

To illustrate this effect more concretely, Fig. 3 plots  $P_R = \tau_L$ ,  $P_L = \tau_R$ , and TMR versus  $V$  for the special example of a symmetric junction with the parameters  $k_{L-} = k_{R-} \equiv k_-$ ,  $k_{L+} = k_{R+} \equiv 10k_-$ , and  $\kappa_0 = 6.4k_-$ , whereby each electrode has the  $V = 0$  polarization  $P_L = P_R = 0.5$ . In this illustration,  $\text{TMR}(V)$  is symmetric because it involves both  $P_L$  and  $P_R$  but  $P_{L,R}(V)$  and the torque coefficients  $\tau_{L,R}(V)$  are not. Although the theory preceding this section assumed small  $V$ , the present discussion makes reasonable the application of the results to finite  $V$  with the understanding that the polarization of the collecting electrode generally depends more strongly on  $V$ . Of course, the toy model cannot make quantitative predictions of the  $V$ -dependence which must rest on details of electron structure [9],[12].

Note that while critical *current density* for magnetic excitation at 0 K is appropriate to junctions with metallic spacers, the high resistance of a MTJ makes critical voltage more appropriate. [Indeed, strictly speaking, the critical current of a *constant-current* generator will generally *differ* from the current density flowing at threshold in the presence of constant external voltage.] In the case of left-right *separability*, valid for  $w \rightarrow \infty$ , one replaces  $\tau_R(V) \rightarrow P_L(V)$  as above and in previous Sections. (The general *inseparable* case is discussed below.)

A significant difference between metallic and insulating spacers lies in the symmetry of the torque. The simple  $\sin\theta$  dependence at constant  $V$  in the tunneling case has no counterpart in the metallic case where more general torque expressions typically contribute to asymmetry of excitation threshold. But the non-ohmic resistance of a tunneling barrier gives rise to the torque asymmetry of  $\tau_R(V)$  exhibited in Fig. 3 which naturally reflects in asymmetry in 0 K voltage threshold. proportional to channel currents.

## 6 Ideal-middle model for separability

A recent publication compares existing theoretical arguments supporting the existence of tunnel-polarization factors [17]. Each of these arguments assumes incident states with conserved crystalline momentum. One argument assumes complete absence of disorder so that the tunneling through a thick barrier is dominated by a single value of lateral momentum. Another is the model of Tsymbal and Petti- for [15] which recovers factorization and therefore the Julliere formula in a strongly disordered single-band tight-binding model. Similarly, the model of Mathon and Umerski attributes the factorization to phase decoherence due to disorder within the barrier [16], [9]. These treatments are augmented with arguments based on the Feyn- man path integral in a disordered barrier [17]. Our treatment below complements these arguments by foregoing lateral momentum quantization completely within the electrodes and IF interfaces while preserving ideal crystalline ordering or vacuum within the middle of the barrier.

We establish sufficient conditions on the hamiltonian  $H$  of Sec.3 for the separa- bility demanded for definition of the polarization coefficients used in the previous sections. The left  $(\psi_{p,\sigma})$  and right  $(\varphi_{q,\sigma'})$  orbital basis functions for the transfer matrix, introduced in Sec. 3, are governed in detail by the general potential  $U_\sigma$  or  $\sigma'$  depending on spin, crystal structure, alloy composition, defects, F/I interface rough- ness and atomic interdiffusion, etc. The quantum numbers  $p$  and  $q$  do not refer to any diagonal operator. Figure 4 indicates the structural scheme. Exceptionally, the *ideal-middle*  $\mathcal{B}$  of the barrier is an ideal crystalline slab or vacuum region defined by  $a \leq x \leq b$  where the planes  $x=a, b$  are dubbed *portals* of the ideal middle. In order to define the left and right basis-state sets of the Bardeen theory, the barrier potential extends into alternative semi-infinite spaces  $(a \leq x)$  and  $(x \leq b)$ , where it is greater than  $\varepsilon_F$ , independent or periodically dependent on  $y, z$  and independent of  $\sigma$  and  $\sigma'$ . The respective conditions  $\psi_{p,\sigma} \rightarrow 0$  for  $x \rightarrow \infty$  and  $\varphi_{q,\sigma'} \rightarrow 0$  for  $x \rightarrow -\infty$  complete the definitions of  $\psi_{p,\sigma}$  and  $\varphi_{q,\sigma'}$ .

The effective-mass theorem [37] is valid when  $\varepsilon$  is near the bottom  $\mathbf{k} = \mathbf{k}_0$  of the conduction band within region  $\mathcal{B}$ . Then the evanescent portion of a left-magnet basis function within this region is approximated by

$$\psi_{p,\sigma} = \Psi_{p,\sigma}(x, y, z) u_{cb, \mathbf{k}_0}(x, y, z) \quad (25)$$

where  $\Psi_{p,\sigma}$  satisfies  $(\mathcal{H}_{\text{bar}} - \varepsilon_{p,\sigma})\Psi_{p,\sigma} = 0$  and  $\Psi_{p,\sigma} \rightarrow 0$  for  $x \rightarrow \infty$ , and  $u_{cb, \mathbf{k}_0}$  is the Bloch function for the bottom of the conduction band. The effective barrier hamiltonian is  $\mathcal{H}_{\text{bar}} = -\hbar^2 \nabla^2 / 2m_{cb} + \mathcal{U}(x)$  where  $m_{cb}$  is the effective mass and  $\mathcal{U}(x)$  ( $> \varepsilon_F$ ) is the spin-independent atomically smoothed effective barrier potential.

Similarly for  $F_R$ ,  $\varphi_{q,\sigma'} = \Phi_{q,\sigma'} u_{cb,k_0}$  with  $\Phi_{q,\sigma'} \rightarrow 0$  for  $x \rightarrow -\infty$ . In case of vacuum,  $\Psi, \Phi$  are indistinguishable from  $\psi, \varphi$ . (Note however that this treatment fails if *both*  $V$  is finite and the FI interfaces are disordered for then  $\mathcal{U}$  depends on  $y$  and  $z$  as well as  $x$ .)

Assuming periodic boundary conditions in  $\boldsymbol{\rho} = (y, z)$  space, the evanescent portions of left and right basis states within  $\mathcal{B}$  are conveniently fourier-expanded in space  $\boldsymbol{\rho}$  with the WKB approximation giving

$$\Psi_{p,\sigma} = \sum_{\mathbf{k}} \lambda_{p,\sigma}(\mathbf{k}) [\kappa(k, a)/\kappa(k, x)]^{1/2} \exp \left[ - \int_a^x \kappa(k, x') dx' + i\mathbf{k} \cdot \boldsymbol{\rho} \right] \quad (26)$$

and

$$\Phi_{q,\sigma'} = \sum_{\mathbf{k}} \mu_{q,\sigma'}(\mathbf{k}) [\kappa(k, b)/\kappa(k, x)]^{1/2} \exp \left[ - \int_x^b \kappa(k, x') dx' + i\mathbf{k} \cdot \boldsymbol{\rho} \right] \quad (27)$$

where the sums  $\sum_{\mathbf{k}}$  are carried over a 2-dimensional reduced Brillouin zone. In these formulas, the function

$$\kappa(k, x) = [\kappa_0^2(x) + k^2]^{1/2}, \quad \text{with } \kappa_0^2 = 2m_{cb}[\mathcal{U}(x) - \varepsilon_F]/\hbar^2, \quad (28)$$

is the imaginary wave-vector in region  $\mathcal{B}$ . Note that Eqs. (26) and (27) reduce to expansions of  $\psi_{p,\sigma}$  and  $\varphi_{q,\sigma'}$  with coefficients  $\lambda_{p,\sigma}(\mathbf{k})$  and  $\mu_{q,\sigma'}(\mathbf{k})$  on the portal planes  $x = a$  and  $x = b$  respectively.

The transfer-hamiltonian matrix element of Eq.(7) is evaluated at any  $x$  lying within the interval  $a \leq x \leq b$ . Consequently  $\Psi, \Phi$ , and  $m_{cb}$  may replace  $\psi, \varphi$ , and  $m$  respectively in this formula. A convenient choice to evaluate Eq. (7) is  $x = x_{\max}$ , satisfying  $\mathcal{U}(x) \leq U(x_{\max})$  for all  $x$ , because the resulting condition  $\partial\kappa_0/\partial x(x_{\max}) = 0$  simplifies the mathematics. (Inclusion in  $\mathcal{U}$  of the image potential due to electron-electron correlation will often insure the presence of a maximum, even if  $|V|$  is large.) Integration over  $y$  and  $z$ , with the assistance of the identity  $\int d\boldsymbol{\rho}^2 \exp[i(\mathbf{k} - \mathbf{k}') \cdot \boldsymbol{\rho}] = \delta_{\mathbf{k},\mathbf{k}'}$ , reduces Eq. (7) to

$$\gamma_{p,\sigma;q,\sigma'} = \sum_{\mathbf{k}} F(\mathbf{k}) \lambda_{p,\sigma}^*(\mathbf{k}) \mu_{q,\sigma'}(\mathbf{k}) \quad (29)$$

where

$$F(\mathbf{k}) = \frac{-4\pi^2\hbar^2}{m_{cb}} \kappa^{1/2}(\mathbf{k}, a) \kappa^{1/2}(\mathbf{k}, b) \exp \left[ - \int_a^b dx \kappa(k, x) \right]. \quad (30)$$

Here we use  $\lambda_{p,\sigma}^*(\mathbf{k}) = \lambda_{p,\sigma}(-\mathbf{k})$  and  $\mu_{q,\sigma'}^*(\mathbf{k}) = \mu_{q,\sigma'}(-\mathbf{k})$  because  $\Psi_{p,\sigma}$  and  $\Phi_{q,\sigma'}$  are real. After rearranging the order of sums, Eq. (10) with (29) and (30) becomes

$$\Gamma_{\sigma,\sigma'} = \frac{2\pi eV}{\hbar} \sum_{\mathbf{k}} F(\mathbf{k}) \sum_{\mathbf{k}'} F(\mathbf{k}') \mathcal{L}_{\sigma}(\mathbf{k}, \mathbf{k}') \mathcal{M}_{\sigma'}(\mathbf{k}, \mathbf{k}') \quad (31)$$

where the two functions

$$\mathcal{L}_\sigma = \sum_p' \lambda_{p,\sigma}^*(\mathbf{k}) \lambda_{p,\sigma}(\mathbf{k}'), \quad \mathcal{M}_{\sigma'} = \sum_q' \mu_{q,\sigma'}(\mathbf{k}) \mu_{q,\sigma'}^*(\mathbf{k}') \quad (32)$$

depend only on parameters of the left and right magnet-and-barrier combinations respectively. The ' on  $\Sigma'$  signifies the conditions given previously for Eq. (8).

Since the sums in Eqs.(32) are carried over many states of randomized character in case of atomic disorder, both have the nature of statistical auto-correlations which should depend smoothly on  $\mathbf{k}$  and  $\mathbf{k}'$ . In the presence of finite atomic disorder they are taylor expandable about  $\mathbf{k} = \mathbf{k}' = 0$ . (See Sec. 5 for the toy free-electron case of vanishing disorder [1] in which one may formally replace  $p \rightarrow \mathbf{k}''$ ,  $q \rightarrow \mathbf{k}'''$  and  $\mathcal{L}_\sigma$  and  $\mathcal{M}_{\sigma'}$  become proportional to  $\delta_{\mathbf{k},\mathbf{k}'}$ .) In addition, with increasing thickness  $w = b - a$  of region  $\mathcal{B}$ , the exponential in Eq.(30) becomes ever more sharply peaked at  $\mathbf{k} = 0$ . Therefore, to leading order in this taylor expansion, the integrations in Eq. (31) tend, for  $w \rightarrow \infty$ , to left-right separation of the form (16) with  $\Omega_{L,\sigma} = \mathcal{L}_\sigma(0,0)$  and  $\Omega_{R,\sigma'} = \mathcal{M}_{\sigma'}(0,0)$ . Written in full, the parameters needed in the general polarization formula (18) are the *basis-state weights*

$$\Omega_{L,\sigma}^\infty = \sum_p \left( \int \int dydz \Psi_{p,\sigma}(\mathbf{x}_{\max}, y, z) \right)^2 \quad (33)$$

$$\Omega_{R,\sigma'}^\infty = \sum_q \left( \int \int dydz \Phi_{q,\sigma'}(\mathbf{x}_{\max}, y, z) \right)^2 \quad (34)$$

where  $\int \int dydz$  is carried over unit junction area. The function  $f$  in Eq. (16) absorbs any spin-independent factors in Eq. (31). *Note that the latter two equations differ generally from the local state density* (or charge density) often cited in connection with tunneling. ( $\text{LSD} \propto \int \int dydz \Psi^2$ ) They reduce to the LSD only in the complete absence of disorder when the two sums reduce to single terms  $\Psi_{\mathbf{k}=0,\sigma}^2$  and  $\Phi_{\mathbf{k}=0,\sigma'}^2$  independent of  $y$  and  $z$ .

## 7 Correction of polarization at finite thickness

The toy free-electron theory, though founded directly on solution of the wave equation in the entire ideal non-disordered FIF system having a flat barrier potential, is correct to leading order in the *exponential* function  $e^{-\kappa w}$  [1]. Bardeen's THT (transfer-hamiltonian technique) calculation for the same model agrees perfectly with its results, as one knew it should from previous non-spin dependent tunneling theory[19].

Let us assume that THT is also correct to the same exponential degree in the case of general electron structure having any degree of atomic disorder treated with the ideal-middle model. The previous section showed that the THT supports tunnel-polarization phenomenology for  $w \rightarrow \infty$  for any degree of disorder in an MTJ. Using THT we derive here corrections to the formulas (18), (33), and (34) for polarization which we find below vary *algebraically*, not exponentially, with  $w^{-1}$ . Therefore these corrections are reliable in spite of this general weakness of the THT.

Further progress requires parametrization of the autocorrelation functions of Eq.(32). Note first the consequence of assuming that the possibly disordered atomic configuration in  $F_L$  produces no electrostatic potential in  $F_R$  and *vice versa*. From Eqs.(26),(27), and (32), in-plane translation of the (disordered) microscopic potential of the *left electrode* according to  $\rho \rightarrow \rho + (B, C)$  where  $(B, C)$  is a periodic-lattice translation of the barrier middle, has the effects, from Eq. (32),  $\mathcal{L}_\sigma \rightarrow \mathcal{L}_\sigma \exp[i(\mathbf{k}' - \mathbf{k}) \cdot (B, C)]$  and  $\mathcal{M}_{\sigma'} \rightarrow \mathcal{M}_{\sigma'}$ . Averaging over all possible such phase changes makes  $\mathcal{L}_\sigma$  and  $\mathcal{M}_{\sigma'}$  diagonal and eliminates all terms with  $\mathbf{k} \neq \mathbf{k}'$  from the double sum in Eq.(31). This equation now becomes

$$\Gamma_{\sigma, \sigma'} = \frac{2\pi eV}{\hbar} \sum_{\mathbf{k}} F^2(\mathbf{k}) \mathcal{L}_\sigma(\mathbf{k}) \mathcal{M}_{\sigma'}(\mathbf{k}) \quad (35)$$

using the now diagonal forms.

In the special case of vanishing disorder, the state indices  $p$  and  $q$  become  $m, \mathbf{k}$  and  $n, \mathbf{k}$  respectively, with  $m, n$  the respective band indices and  $\mathbf{k}$  the lateral crystalline momentum. Let the basis states be normalized to unity. Then the diagonal elements of formulas (32) reduce to

$$\mathcal{L}_\sigma = \sum_m |\lambda_{m, \sigma}(\mathbf{k})|^2 / v_{x, m, \sigma}(\mathbf{k}) , \quad \mathcal{M}_{\sigma'} = \sum_n |\mu_{n, \sigma'}(\mathbf{k})|^2 / v_{x, n, \sigma'}(\mathbf{k}) \quad (36)$$

with factors independent of  $\sigma$  and  $\sigma'$  omitted. Here  $v_{x, m, \sigma} = \partial \varepsilon_{m, \sigma}(\mathbf{k}) / \partial k_x$  and  $v_{x, n, \sigma'} = \partial \varepsilon_{n, \sigma'}(\mathbf{k}) / \partial k_x$  are velocity components normal to the junction plane. Their presence in these formulas follows from the restriction on  $\Sigma'$  in the basic formula (8).

To evaluate Eq. (35) for general disorder, specialize to small  $V$  and constant  $\mathcal{U}$  inside  $\mathcal{B}$ . After evaluation of the integral in Eq. (30), it reduces to the form

$$\Gamma_{\sigma, \sigma'} = f_1 \sum_{\mathbf{k}} \kappa^2(\mathbf{k}) e^{-2w\kappa(\mathbf{k})} \mathcal{L}_\sigma(\mathbf{k}) \mathcal{M}_{\sigma'}(\mathbf{k})$$

where  $f_1$  does not depend on  $\sigma$  or  $\sigma'$ .

For large  $w$ , this sum weights small  $k$  heavily. Therefore parametrize  $\mathcal{L}_\sigma$  and  $\mathcal{M}_{\sigma'}$  for small  $k$  with the lateral spatial *correlation scales*  $(\xi_\sigma, \eta_{\sigma'})$  defined by the

formulas

$$\begin{aligned}\mathcal{L}_\sigma(\mathbf{k}) &= \mathcal{L}_\sigma(0)[1 - \xi_\sigma^2 k^2 + \mathcal{O}(k^4)], \\ \mathcal{M}_{\sigma'}(\mathbf{k}) &= \mathcal{M}_{\sigma'}(0)[1 - \eta_{\sigma'}^2 k^2 + \mathcal{O}(k^4)]\end{aligned}\tag{37}$$

and approximate Eq.(28) with  $\kappa \approx \kappa_0 + (k^2/2\kappa_0)$  in the exponent of Eq.(30). After approximating  $\sum_{\mathbf{k}}$  (over one BZ) with an infinite integral, one finds correctly to first order in  $w^{-1}$

$$\Gamma_{\sigma,\sigma'} = f_2 \mathcal{L}_\sigma(0) \left(1 - \frac{\kappa_0 \xi_\sigma^2}{w + \kappa_0^{-1}}\right) \mathcal{M}_{\sigma'}(0) \left(1 - \frac{\kappa_0 \eta_{\sigma'}^2}{w + \kappa_0^{-1}}\right)\tag{38}$$

where once again factors independent of both  $\sigma$  and  $\sigma'$  are absorbed into  $f_2$ . Thus to this approximation,  $\Gamma_{\sigma,\sigma'}$  once again has the factored form (16). The corrected left polarization factor, according to Eq.(18) reduces upon expansion to

$$\begin{aligned}P_L &= P_L^\infty + \frac{1}{2} (1 - P_L^\infty)^2 \frac{\kappa_0(\xi_-^2 - \xi_+^2)}{w + \kappa_0^{-1}} + \dots \quad \text{with} \\ P_L^\infty &= \frac{\Omega_{L,+}^\infty - \Omega_{L,-}^\infty}{\Omega_{L,+}^\infty + \Omega_{L,-}^\infty},\end{aligned}\tag{39}$$

where  $\Omega_{L,\pm}^\infty$  are given by Eq. (33), and similarly for  $P_R$ . Thus, for given Bardeen basis functions one has polarization factors correctly to order  $w^{-1}$ .

## 8 Summary and Discussion

Although it is valid only in the limit of weak transmission[18], predictions from Bardeen's tunneling theory are interesting because it does not require electron momentum in the electrodes to be conserved. Our application to elastic tunneling in ordered or disordered magnetic tunneling junctions yields these new conclusions:

- In Section 3 we found that the voltage-driven pseudo-torque at constant external *voltage* is generally proportional to  $\sin \theta$  [Eq.(15)] . This contrasts with the variable angular dependence conditioned on electron structure and resistance parameters in the case of a metallic spacer [20]. In general, polarization factors do not exist in the absence of special assumptions, in agreement with previous theory[9],[12].

- In Section 4 we found that if the polarization factors *are* well defined, then at constant applied voltage the angular dependences of current and torque obey the simple relations of Eqs. (3) [14], (19), and (20). These predictions are satisfied by those derived by direct solution of the Schroedinger equation for the toy model of parabolic bands and ideal rectangular potential barrier without any disorder[1].
- Experimentally, TMR is known to usually diminish with increasing external voltage  $V$  [9], [10]. In Section 5 we considered that it is the polarizing factor of the collector electrode which decreases more strongly with  $V$  [31], resulting in the unsymmetric schematic pattern of voltage dependence of torque indicated in Fig. 3. This lack of symmetry due to the relations  $\tau_R = P_L$  and  $\tau_L = P_R$  implies that the threshold voltage for switching initiation will be increasingly asymmetric at the higher values ( $>100$  mV) likely needed for writing in memory. Cases may well arise in which voltage-driven switching works in only one direction. Experimentally, for selected junctions switching occurs at a voltage sufficiently high for TMR to become negligible [7]. Our Fig. 3 indicates how this may happen at 0 K for switching in but one direction, from AP to P. However, it would not explain any *symmetric* persistence of switching at voltages great enough to destroy TMR.
- Our approach to the validation of polarization factors complements previous studies which accounted for atomic disorder in the barrier assuming incident states with well-defined crystalline momentum [15], [16],[17]. So long as the barrier is thick and *internally* crystalline (or vacuum) as in Fig. 4, then a newly derived  $w \rightarrow \infty$  polarization factor, given by Eqs. (18), (33), and (34), is valid even in the presence of great disorder in the electrodes and interfacial disorder sufficient to destroy the conservation of lateral crystalline momentum throughout the electrode and interface regions. This polarization factor generally depends not merely on the chemical composition of the magnet but its state of atomic disorder as well as that of the F/I interface. The key basis-state weight factors (33) and (34) are more general than conventional local state density.
- Our conclusion that polarization factors are more valid with increasing  $w$  tends to undermine our predictions of voltage asymmetry of torque shown in Fig. 3. For experimental torque effects such as switching will require thin barriers for which the separability condition on which Fig. 3 is based is less valid.
- Our parametrized expression (39) for dependence of tunnel polarization on



ideal-middle thickness  $w$  is without precedent. A strong dependence is expected from certain compositions, like Co, Ni, and certain alloys, such as FeCo, lying on the negative-slope region of the Slater-Pauling curve; for their strong contrast between the heavily 4sp density of majority-spin and the heavily 3d density of minority-spin bands may be reflected in strongly contrasting magnitudes of lateral autocorrelation scales  $\xi_+$  and  $\xi_-$ .

- In fact, experimental junctions having composition Fe/Al<sub>2</sub>O<sub>3</sub>/FeCo show dependence of TMR on  $w$  [10] at T=2 K where our assumption of elastic tunneling should be valid. The expected monotonic dependence on thickness is observed for two crystallographic orientations on single-crystal Fe, but not on the third. Although the R electrode (FeCo) lies on the negative-slope, the L electrode (Fe) lies on the positive-slope side of the Slater-Pauling curve where high 3d density exists for both signs of spin so that there may be little difference between  $\xi_+$  and  $\xi_-$ . Junctions with both electrodes taken from the negative-slope side may yield a more pronounced thickness dependence of TMR on barrier thickness according to the present theory.

**Acknowledgments.** The author is grateful for helpful discussions with W. Butler, E. Tsymbal, M. Stiles, Y. Bazaliy, J. Sun, S. S. P. Parkin, P. Nguyen, G. Fuchs, D. Worledge, and P. Visscher.

## References

- [1] J. C. Slonczewski, Phys. Rev. B, **39**, 6995 (1989).
- [2] S. I. Kiselev *et al*, Nature , **425**, 380 (2003).
- [3] W. H. Rippard, M. R. Pufall, S. Kaka, S. E. Russek, and T. J. Silva, Phys. Rev. Lett. **92**, xxxx(2004).
- [4] J. S. Moodera, L. R. Kinder, T. M. Wong, and R. Meservey, Phys. Rev. Lett. **74**, 3273 (1995).
- [5] S. S. P. Parkin, in *Spin Dependent Transport in Magnetic Nanostructures* (Taylor & Francis, 2002), p. 237.
- [6] Y. Huai, F. Albert, P. Nguyen, M. Pakala, and T. Valet, Appl. Phys. Lett. **84**, xxx (2004).
- [7] G. D. Fuchs, N. C. Emley, I. N. Krivorotov, P. M. Braganca, E. M. Ryan, S. I. Kiselev, J. C. Sankey, J. A. Katine, D. C. Ralph, R. A. Buhrman, cond-mat/0404002 (2004).

- [8] J. Slonczewski, Frontiers in Magnetism 99. Stockholm, 12-15 August, arXiv: cond-mat/0205055
- [9] J. S. Moodera and G. Mathon, J. Mag. Mag. Mats. **200**, (1999) 248.
- [10] T. Miyazaki, Chapter 3 in *Spin Dependent Transport in Magnetic Nanostructures*, edited by S. Maekawa and T. Shinjo (Taylor & Francis, 2002).
- [11] S. Maekawa, S. Takahashi, and H. Imamura, Chapter 4 in *Spin Dependent Transport in Magnetic Nanostructures* (Taylor & Francis, 2002).
- [12] E. Y. Tsymbal, O. N. Mryasov, and P. R. LeClair, J. Phys.: Condens. Matter **15**, R109 (2003).
- [13] R. Meservey and P. M. Tedrow, Physics Reports **238**, 173 (1994).
- [14] M. Julliere, Phys. Lett. **54A**, 225 (1975).
- [15] E. Y. Tsymbal and D. G. Pettifor, Phys. Rev. B **58**, 432 (1998).
- [16] J. Mathon and A. Umerski, Phys. Rev. B **60**, 1117(1999).
- [17] K. D. Belashchenko, E. Y. Tsymbal, M. van Schilfgaarde, D. A. Stewart, I. I. Oleynik, and S. S. Jaswal, arXiv: cond- mat/ 0308268 v2, 15 Dec 2003
- [18] J. Bardeen, Phys. Rev. Letts. **6**, 57 (1961).
- [19] C. B. Duke, *Tunneling in Solids*, (Academic Press, New York, 1969).
- [20] J. Slonczewski, J. Magn. Magn. Mater. **247** (2002) 324.
- [21] L. Berger, Phys. Rev. B **54** (1996) 9353.
- [22] Y. B. Bazaliy, B. A. Jones, and S.-C. Zhang, Phys. Rev. B **57** (1998) R3213.
- [23] J. Slonczewski, J. Magn. Magn. Mats. **195** (1999) L261.
- [24] M. D. Stiles and A. Zangwill, Phys. Rev. B **66**, 014407 (2002).
- [25] F. J. Albert, N. C. Emley, E. B. Myers, D. C. Ralph, and R. A. Buhrman, Phys. Rev. Lett. **89**, 226802(2002).
- [26] J. Bass and W. P. Pratt, Jr., J. Magn. Magn. Mats. **200** (1999) 274.
- [27] J. Kübler, *Theory of Itinerant Electron Magnetism* (Oxford Science Publications, 2000), p. 234.
- [28] T. Valet and A. Fert, Phys. Rev. B **48** (1993) 7099.
- [29] Eq. (18.34) in Ref. [19].
- [30] N. Tezuka and T. Miyazaki, J. Magn. and Magn. Mats. **177-181**, 1283 (1998).

- [31] Jun Du, Fei-fe Li, Zheng-Zhong Li, Ming-wen Xiao, Wang Xu, and An Hu, 9th Joint MMM/Intermag Conference, Anaheim, Jan. 5-9, 2004, Abst. FT-01.
- [32] J. A. Katine, F. J. Albert, R. A. Buhrman, E. B. Myers, and D. C. Ralph, Phys. Rev. Lett. **84** (2000) 3149.
- [33] J. Z. Sun, Phys. Rev. B **62**,570 (2000).
- [34] Ya. B. Bazaliy, B. A. Jones, and S. C. Zhang, J. Appl. Phys. **89** (2001) 6793.
- [35] Thierry Valet, private communication
- [36] J. C. Slonczewski, J. Magn. and Magn. Mats. **159**, L1 (1996).
- [37] See, for example, A. C. Smith, J. F. Janak, and R. S. Adler, *Electronic Conduction in Solids* (McGraw-Hill 1967) p. 125.

# Figure Captions

Fig. 1. (a) Scheme of magnetic tunnel junction and key to notations. (b) Equivalent circuit for spin-channel currents and further key to notations.

Fig. 2. Schematic junction potential for finite  $V$ . The shaded bar indicates the energy range of most of the tunneling electrons.

Fig. 3. Schematic effect of finite voltage on TMR, polarization, and torque coefficients illustrated by the toy free electron model of a symmetric magnetic tunnel junction. TMR is symmetric but the other coefficients are not. Case  $P_L = P_R = 0.5$ ,  $k_+ = 10k_-$ .

Fig. 4. Depiction of the ideal-middle model of a magnetic tunneling junction. Disorder without limit is permitted in both electrodes and barrier except within a central slab  $\mathcal{B}$  of the barrier lying between the portal planes  $x = a, b$ .

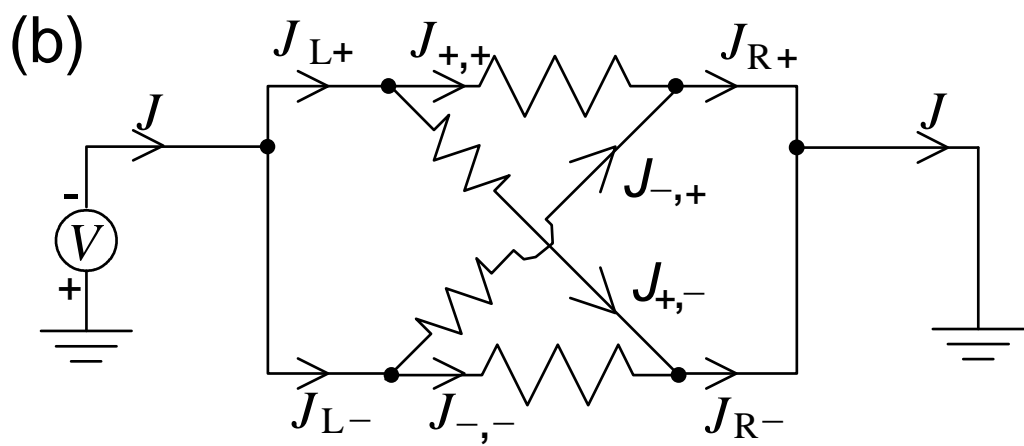
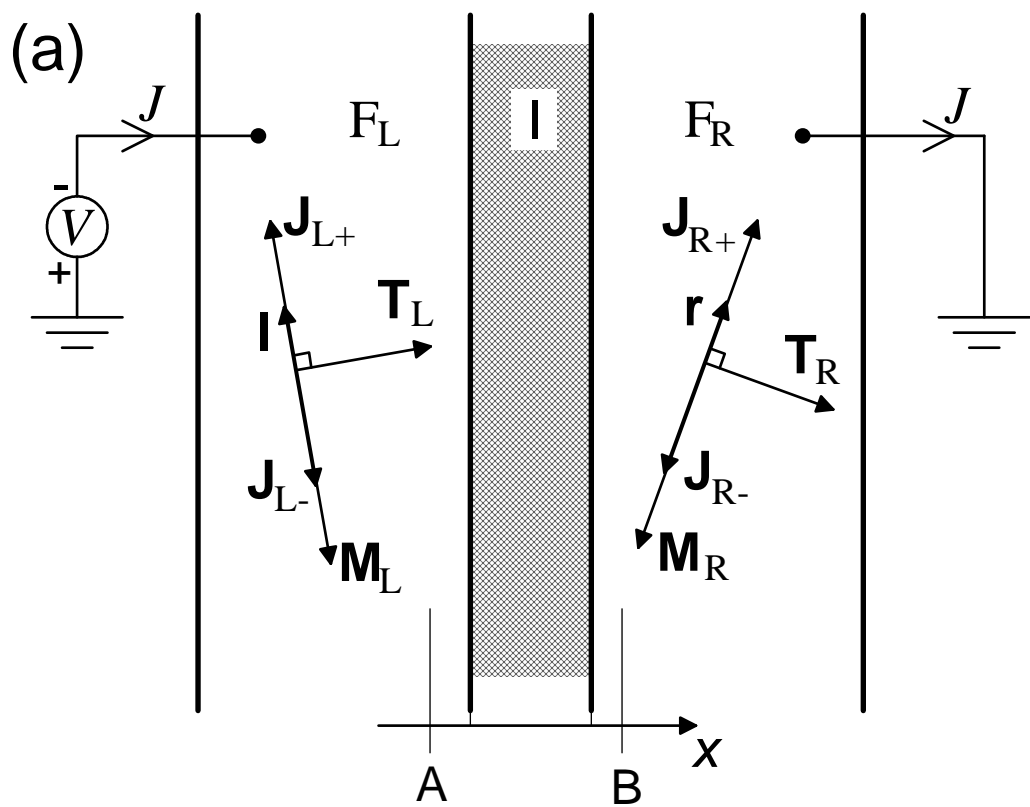


Fig. 1

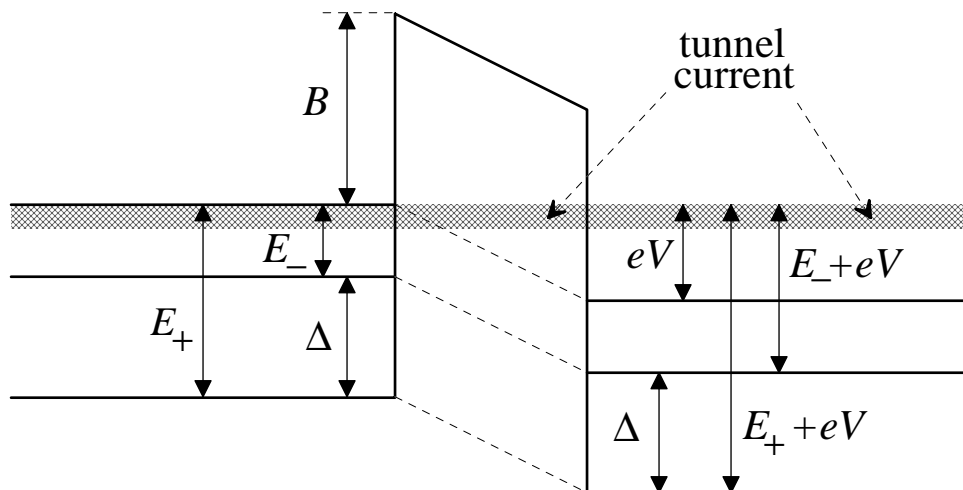


Fig. 2

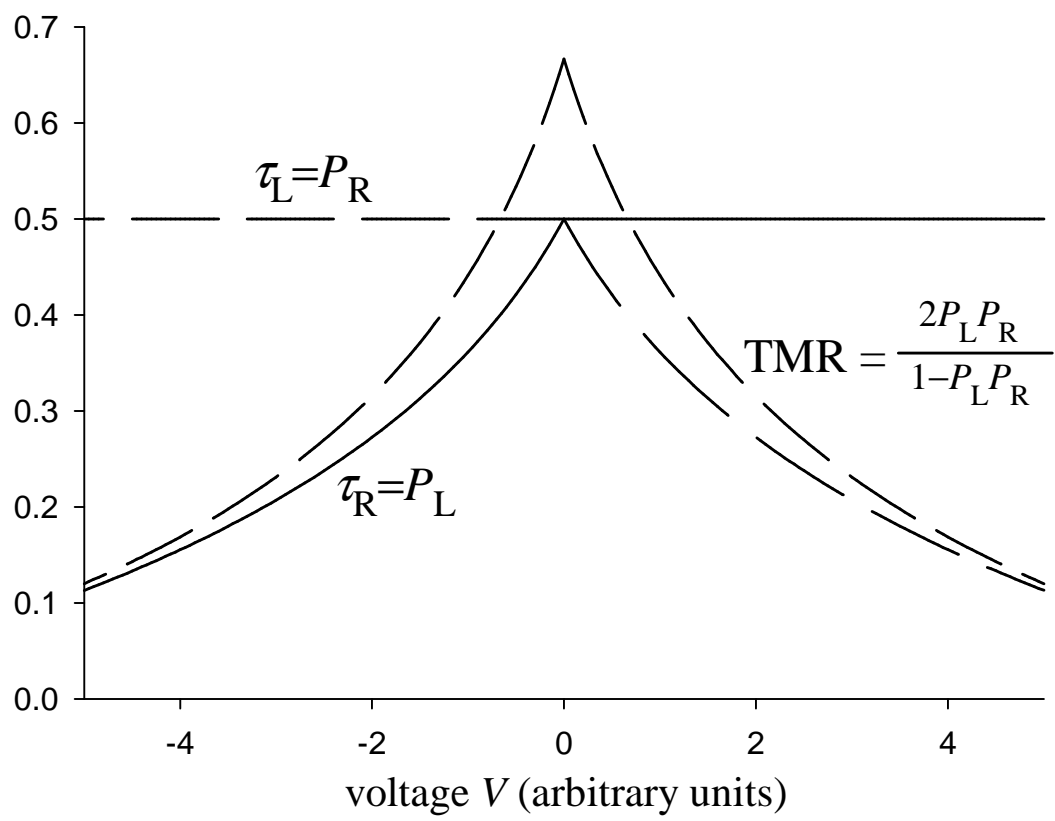


Fig. 3

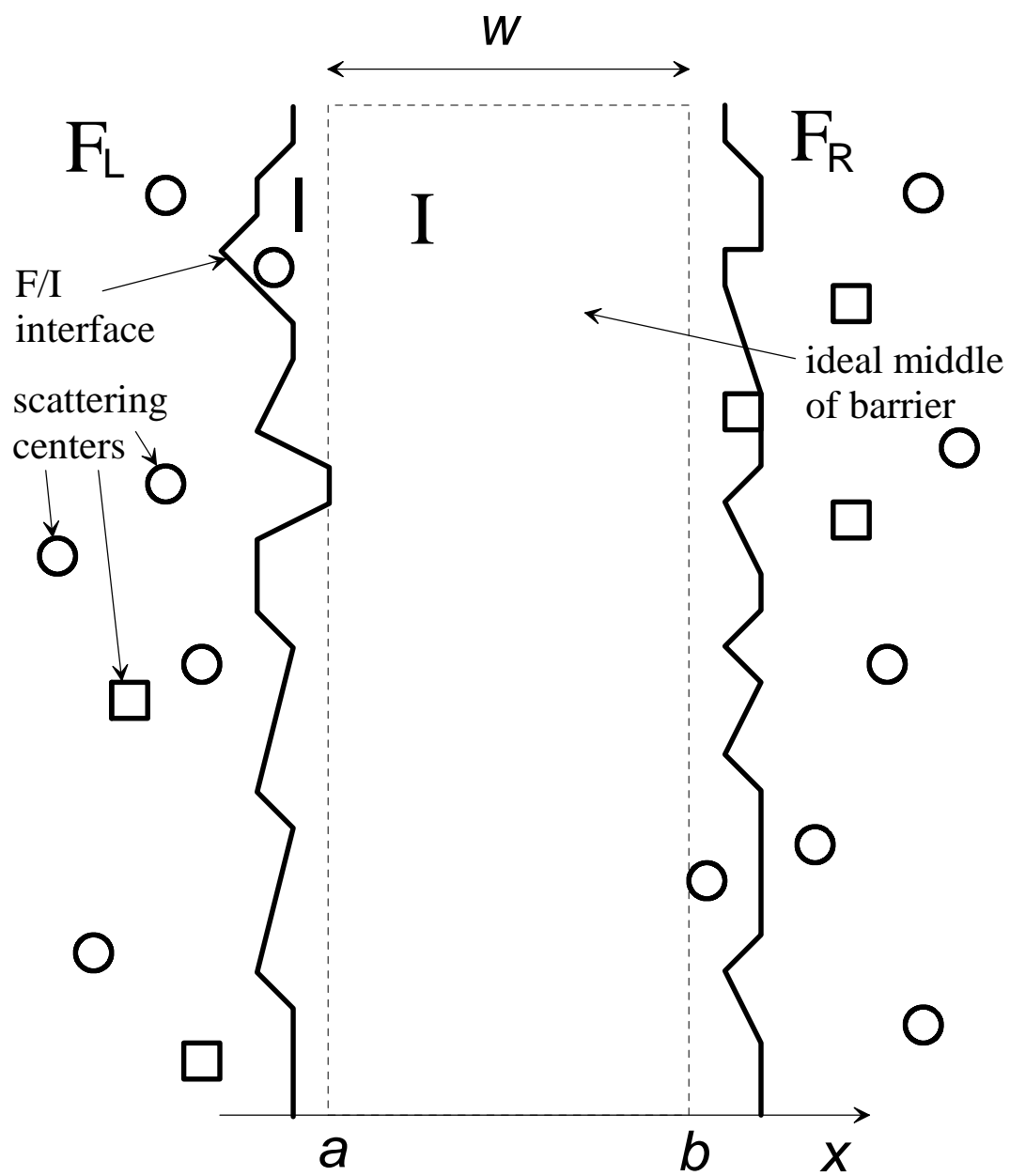


Fig. 4